Synthesis of New Dehydrodieugenol Derivatives via Olefin Cross Metathesis and In Vitro Evaluation of Their Trypanocidal Activity

Thalita S. Galhardo, Anderson K. Ueno, Wagner A. Carvalho, Thaís A Costa-Silva, Marina M. Goncalves, Mariana B. Abiuzi, Andre G. Tempone, João Henrique G Lago, Dalmo Mandelli, Cedric Fischmeister, et al.

catalysts

MDPI

Article

Synthesis of New Dehydrodieugenol Derivatives via Olefin Cross Metathesis and In Vitro Evaluation of Their Trypanocidal Activity

Thalita S. Galhardo [1], Anderson K. Ueno [2], Wagner A. Carvalho [1], Thais A. Costa-Silva [1], Marina M. Gonçalves [1], Mariana B. Abiuzi [3], Andre G. Tempone [3], João Henrique G. Lago [1,*], Dalmo Mandelli [1], Cedric Fischmeister [4,*] and Christian Bruneau [4]

[1] Center for Natural and Human Sciences, Federal University of ABC, Santo André 09210-180, Brazil; thata.galhardo@gmail.com (T.S.G.); wagner.carvalho@ufabc.edu.br (W.A.C.); tha_isbio@yahoo.com.br (T.A.C.-S.); marina.monroe@ufabc.edu.br (M.M.G.); dalmo.mandelli@ufabc.edu.br (D.M.)
[2] Institute of Environmental, Chemical, and Pharmaceutical Sciences, Federal University of São Paulo, Diadema 09972-270, Brazil; ueno.unifesp@gmail.com
[3] Center for Parasitology and Mycology, Instituto Adolfo Lutz, São Paulo 01246-902, Brazil; mariana.abiuzi@gmail.com (M.B.A.); andre.tempone@ial.sp.gov.br (A.G.T.)
[4] Institut des Sciences Chimiques de Rennes (ISCR)—UMR 6226, Université de Rennes, Centre National de la Recherche Scientifique (CNRS), 35042 Rennes, France; christian.bruneau@univ-rennes.fr
* Correspondence: joao.lago@ufabc.edu.br (J.H.G.L.); cedric.fischmeister@univ-rennes.fr (C.F.)

Abstract: Ruthenium-catalyzed cross metathesis using biseugenol (**1**) with electron-deficient olefins methyl (**2a**) and ethyl (**2b**) acrylates, acrylic acid (**2c**), acrylonitrile (**2d**), and methyl methacrylate (**2e**) derivatives have been conducted to afford respective derivatives **3a**–**3e** with good yields and excellent conversion rates. Activity of prepared compounds against trypomastigote and amastigote forms of *Trypanosoma cruzi* and mammalian cytotoxicity have been evaluated. The results obtained indicate that the IC_{50} values for amastigotes of compounds **3b** and **3d** are quite similar to those of biseugenol (**1**), but unlike this compound, they show reduced toxicities with SI values similar to those of the standard drug benznidazol.

Keywords: dehydrodieugenol; olefin cross metathesis; ruthenium; anti-trypanosomal activity; *Trypanosoma cruzi*

Citation: Galhardo, T.S.; Ueno, A.K.; Carvalho, W.A.; Costa-Silva, T.A.; Gonçalves, M.M.; Abiuzi, M.B.; Tempone, A.G.; Lago, J.H.G.; Mandelli, D.; Fischmeister, C.; et al. Synthesis of New Dehydrodieugenol Derivatives via Olefin Cross Metathesis and In Vitro Evaluation of Their Trypanocidal Activity. *Catalysts* **2023**, *13*, 1097. https://doi.org/10.3390/catal13071097

Academic Editor: Kotohiro Nomura

Received: 19 June 2023
Revised: 11 July 2023
Accepted: 11 July 2023
Published: 13 July 2023

1. Introduction

Over the last decade, natural products have been one of the most important references in drug discovery and development [1]. Indeed, over the last 30 years, half of all the new medicines introduced were based on natural products, which underlines their importance for lead generations [2,3]. After all, these compounds produced by nature are the result of millions of years of evolutionary selection and are therefore biologically pre-validated. All these factors have led to the validation of natural products as prime starting points for drug discovery.

Phenylpropanoid derivatives such as eugenol, isoeugenol, and their dimeric compounds (lignoids) correspond to an important class of natural products found in medicinal plants [4,5]. Consequently, these compounds have attracted considerable attention in the pharmaceutical industry due to their pharmacological potential. On the other hand, eugenol (the main component in clove oil), is a valuable starting compound for several drugs. It has been used in cosmetics and food products as a flavoring additive, antimicrobial, and antioxidant agent [6], as well as in dentistry where it is used in combination with zinc oxide as a pulp capping agent, temporary filling, and root conduit sealer [7].

However, eugenol causes allergenic contact dermatitis [8,9] and high concentrations of this compound have been reported to have some cytotoxic properties [10].

Biseugenol, also known as dehydrodieugenol (**1**), a symmetrical dimer of eugenol, is a natural product [11] which shows antioxidant [12,13] and anti-inflammatory [14,15] biological activity but with reduced cytotoxicity in comparison to eugenol [16]. The o-hydroxylated biphenyl structure found in the structure of compound **1** also exists in a large number of naturally occurring compounds, such as magnolol and honokiol, which have important pharmacological properties [17–19]. Furthermore, many studies have shown that compound **1** exhibits antineoplasic [20], antimicrobial [21,22], anti-inflammatory [23], antiarthritic [24], and antiproliferative activities [25]. It is also an apoptosis-inducing agent [26,27]. Bioactivity assays of natural biseugenol extracted from clove (*Syzygium aromaticum*) buds indicate antimutagenic activity [28], induction of cytotoxicity and apoptosis, inhibition of COX-2 gene expression [29], ability to treat cancer and other neoplasms [30], and possible inhibition of NFjB [14]. Additionally, chemical studies performed with Brazilian plant species *Nectandra leucantha* afforded compounds **1** and its methylated derivative which were evaluated in vitro against *Trypanosoma cruzi* [31]. As described, the presence of the phenol group was found to be crucial to the antiparasitic potential of compound **1** (IC_{50} values of 11.5 and 15.1 μM to trypomastigote and amastigote forms, respectively) but responsible for mammalian cytotoxicity (CC_{50} of 58.2 μM). On the other hand, methylated derivative exhibited reduced activity against *T. cruzi* (IC_{50} of 55.6 and >100 μM to trypomastigote and amastigote forms, respectively) and no toxicity to NCTC cells (CC_{50} > 200 μM).

As well as the modification of the substituent in the phenyl rings, it is possible to modify the allylic carbon-carbon double bond present in these neolignans when aiming at improving their biological activity. Miyazawa and Hisama found that the functionalization of the eugenol double bond induced a higher efficiency in inhibiting mutations that lead to the development of cancer [28]. Regarding this aspect, olefin metathesis could be considered an attractive way to transform these natural products since this process involves an efficient formation of new carbon-carbon double bonds [32]. Moreover, olefin metathesis reactions generally take place under mild reaction conditions, so this catalytic transformation has rapidly become an important synthetic tool for the production of biologically active organic molecules [33] and in total syntheses of natural products [33,34]. Due to their high tolerance to functional groups and robustness towards air and moisture, ruthenium complexes have been selected as catalysts of choice for these transformations. In particular, cross metathesis represents one type of bimolecular olefin metathesis process that has been used for the preparation of natural products such as prosophylline, lasiol, faranal, and meayamycin B [35–37]. Previous studies reporting the total synthesis of Δ^{12}-prostaglandin, which displayed potent anticancer activity [38], as well as jasmonic acid derivatives, responsible for defense reactions after wounding or pathogen infestation [39], represent relevant examples of synthesis of biologically active molecules accomplished via olefin cross metathesis. Previous studies using eugenol in cross metathesis reactions with a variety of alkenes for the preparation of biologically active molecules have been reported [40,41]. Our group reported that eugenol was favorably involved in cross metathesis reactions in the presence of ruthenium catalysts allowing its straightforward functionalization [42–44]. More recently, dehydrodieugenol B and its methyl ether, both isolated from *Nectandra leucantha*, were used as starting materials for the preparation of new derivatives containing additional methoxycarbonyl units on allyl side chains and demonstrated activity against trypomastigotes and against intracellular amastigotes of *Trypanosoma cruzi* [45]. Based on these results and our knowledge of metathesis for the preparation of biologically active derivatives of eugenol, we report herein the preparation via cross metathesis with functional olefins of novel dehydrodieugenol derivatives **3a**–**3e** using compound **1** as a starting material (Figure 1). We have evaluated the effect of the introduction of different functionalities of the allyl fragment on the biological activity of these new compounds against *Trypanosoma cruzi* (trypomastigote and intracellular amastigote forms).

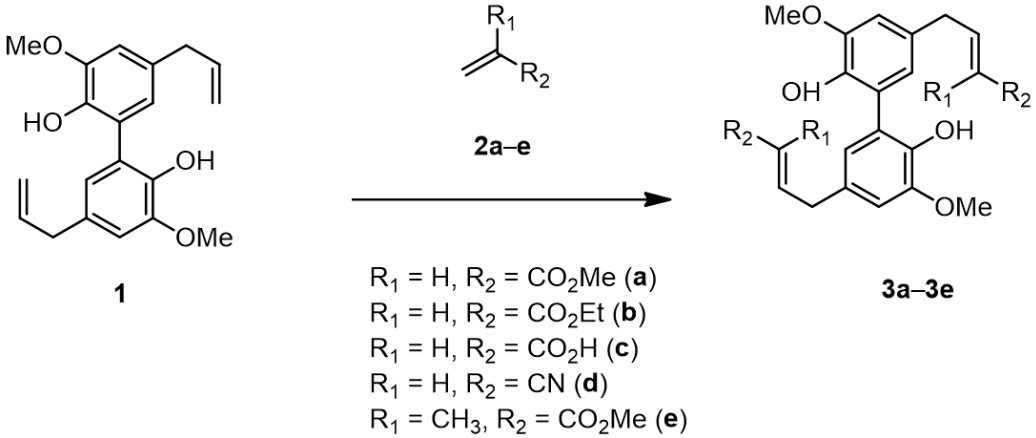

Figure 1. Biseugenol (**1**), olefins **2a**–**2e**, and cross metathesis products **3a**–**3e**.

2. Results and Discussion

The synthesis of biseugenol **1** was achieved via the oxidative coupling of eugenol in the presence of $K_3[Fe(CN)_6]$ as oxidant [46], and led to a 36% isolated yield of **1** with high purity after recrystallization (see experimental section). We have previously shown that the cross metathesis of eugenol with acrylates [42–44] was efficiently carried out in the presence of the second generation Hoveyda ruthenium catalyst **Ru1** [47]. The isomerization of allylbenzene derivatives including 4-hydroxyphenylpropanoids in the presence of ruthenium olefin metathesis catalysts has been extensively described by van Otterlo [48], who suggested that the utilization of an isomerization inhibitor should be recommended to avoid this competing reaction leading to undesired metathesis products. From Figure 2, it appears that the cross metathesis of **1** with electron-deficient olefins should involve two successive steps leading to the mono cross metathesis products, the precursors of the di cross metathesis products **3a**–**3e**.

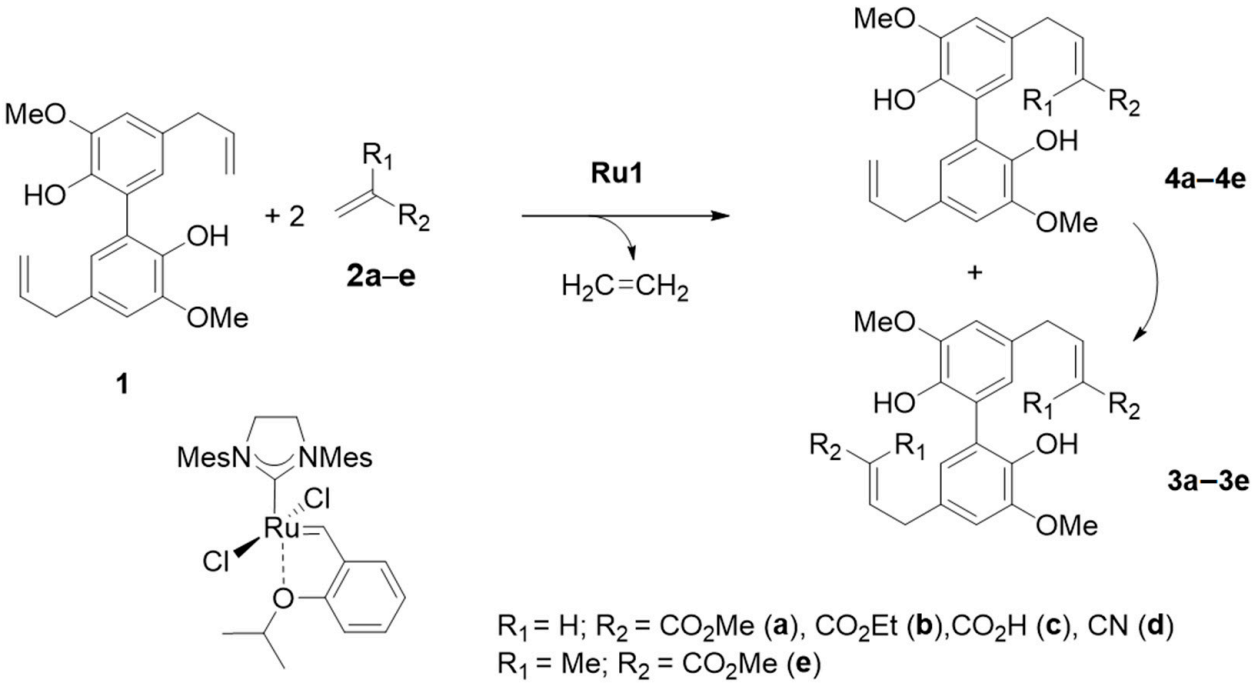

Figure 2. General scheme for cross metathesis of biseugenol **1**.

In some experiments, we could intercept compounds **4a**–**4e**, which proved to be very useful to get information on the characterization of this intermediate, especially the ^1H NMR spectra, and evaluate the efficiency of the different catalytic systems that were tested.

From the reaction with methyl methacrylate, the ^{1}H NMR spectra shows that the signals of the five allylic protons present exactly the same chemical shifts in **4e** as in substrate **1**. Similarly, the aromatic and the hydroxyl protons in substrate **1** and products **3e** and **4e** appear at the same chemical shifts. Consequently, when they are present, the signals of the terminal protons of the allylic system in the region at δ 5.0–5.5 ppm in the crude reaction mixtures do not give information on the nature and ratio of the products **3** or **4** (see Supporting Information). We determined the conversion of **1** with the aid of the integration of the signals of the two terminal CH_2 protons in the range at δ 5.0–5.2 ppm and the methoxy group at δ 3.9 ppm, which led to a conversion lower than the real one due to the impact of the presence of the intermediate **4** in the determination of the terminal allylic protons.

We started the investigations with methyl acrylate **2a** as cross metathesis partner using the conditions that we previously optimized for the cross metathesis with eugenol [42–44]. Our first attempts were made at 80 °C in dimethyl carbonate [49] in the presence of 10 mol% of *p*-benzoquinone as an olefin isomerization inhibitor with 2 mol% of **Ru1** as catalyst and a twofold molar excess of methyl acrylate (Table 1).

Table 1. Cross metathesis of biseugenol **1** with methyl acrylate (**2a**) [a].

Entry	2a (Eq.)	DMC (mL)	Ru1 (mol%)	Time (h)	Conversion (%)
1	4	2	2	16	91
2	4	2	2	(2 + 3) [b]	96
3	4	2	4	(2 + 3) [b]	97
4	12	2	2	(2 + 3) [b]	96
5	4	10	2	(2 + 3) [b]	87

[a] General conditions: **1** (0.15 mmol), T = 80 °C, *p*-benzoquinone (10 mol%); [b] slow addition of the catalyst (0.25 mL/h). Eq. = equivalent; DMC = dimethyl carbonate.

The batch reaction with a **2a/1** molar ratio of four with a biseugenol concentration of 0.075 mol/L in DMC provided 91% conversion of **1** after 16 h (Table 1, entry 1). Then, we used a protocol based on the slow addition of the catalyst into the reaction mixture, which consisted in the addition of the catalyst dissolved in 0.5 mL of solvent over 2 h using a syringe pump followed by 3 h of stirring with these two steps being performed at 80 °C. This process led to an improved conversion of 96% while reducing the reaction time from 16 h to 5 h (Table 1, entry 2). Increasing the catalyst loading or excess of methyl acrylate had no significant effect on the conversion (Table 1, entries 3 and 4), whereas dilution to 0.015 mol/L had a deleterious impact (Table 1, entry 5). Overall, the slow addition of the catalyst for 2 h followed by 3 h of reaction provided the best conditions with a conversion of 96% and only eventually traces of **4a** (≤4%) leading to the isolation of **3a** in 52% yield.

The ^{1}H NMR analysis of the crude reaction mixture after elimination of the solvent and the excess of methyl acrylate (**2a**) not only gave an indication on the conversion of the substrate **1** but also provided information on the configuration of the formed carbon-carbon double bond. Indeed, only one stereoisomer was detected and the value of the coupling constant of 15.6 Hz between the two olefinic protons indicated that the cross metathesis was (*E*)-selective. It is noteworthy that this (*E*) stereoselectivity is perfectly in line with that observed during cross metathesis of **2a** with the monomeric eugenol [42–44].

The cross metathesis of **1** with ethyl acrylate **2b** was conducted under the optimized conditions leading to a conversion of 94%. However, the product was difficult to isolate and only 25% yield could be obtained after purification (Table 2, entry 2). Acrylic acid (**2c**) was involved as cross metathesis partner in order to prepare a new biseugenol derivative featuring carboxylic acid groups (**3c**). These latter are expected to bring new properties in terms of acidity and solubility in aqueous media able to enhance biological activity. Under the catalytic conditions used for the syntheses of **3a** and **3b**, the reaction took place even though the conversion was lower (71%). The resulting diacid **3c** was isolated as a

solid in 32% yield and the reaction exhibited the same high (*E*) stereoselectivity (Table 2, entry 3). The metathesis reactions with acrylonitrile in the presence of second-generation ruthenium catalysts such as **Ru1** are known to require more drastic conditions [50–52]. For this reason, the cross metathesis of **1** with **2d** was carried out in diethyl carbonate at 100 °C. A good conversion of **1** of 88% was obtained and the product **3d** was isolated in 51% yield (Table 2, entry 4). As expected, the use of acrylonitrile did not promote the selective formation of the (*E*) isomer but produced a mixture of the two stereoisomers with a (*Z*)/(*E*) ratio of 2.5:1 based on the ^{1}H NMR analysis of the allylic CH_2 protons at δ 3.72 (*Z*-isomer) and 3.51 (*E* isomer), respectively [53,54]. Then, we investigated the behavior of the α,α-disubstituted methyl methacrylate **2e** under the conditions that were previously optimized with eugenol [42–44]. Without additional solvent, the cross metathesis reaction took place in an excess of **2e** at 90 °C for 16 h without using the slow addition protocol. The conversion of **1** reached 81% and **3e** was isolated in 29% yield as a single (*E*)-stereoisomer (Table 2, entry 5). Structures of compounds **3a**–**3e** are presented in Figure 3.

Table 2. Cross metathesis of **1** with electron deficient olefins **2a**–**2e** [a].

Entry	Substrate	Olefin	Product	Conversion (%)	Yield (%)
1	**1**	Methyl acrylate (**2a**)	**3a**	96	52
2	**1**	Ethyl acrylate (**2b**)	**3b**	94	25
3	**1**	Acrylic acid (**2c**)	**3c**	71	32
4 [b]	**1**	Acrylonitrile (**2d**)	**3d**	88	51
5 [c]	**1**	Methyl methacrylate (**2e**)	**3e**	81	29

[a] Conditions: DMC (2 mL), *p*-benzoquinone (10 mol%), **Ru1** (2 mol%), slow addition of the catalyst (0.25 mL·h^{-1}) (2 + 3 h), T = 80 °C; [b] DEC (2 mL) and T = 100 °C; [c] without solvent (2 mL of methyl methacrylate), T = 90 °C, 16 h, single addition of the catalyst.

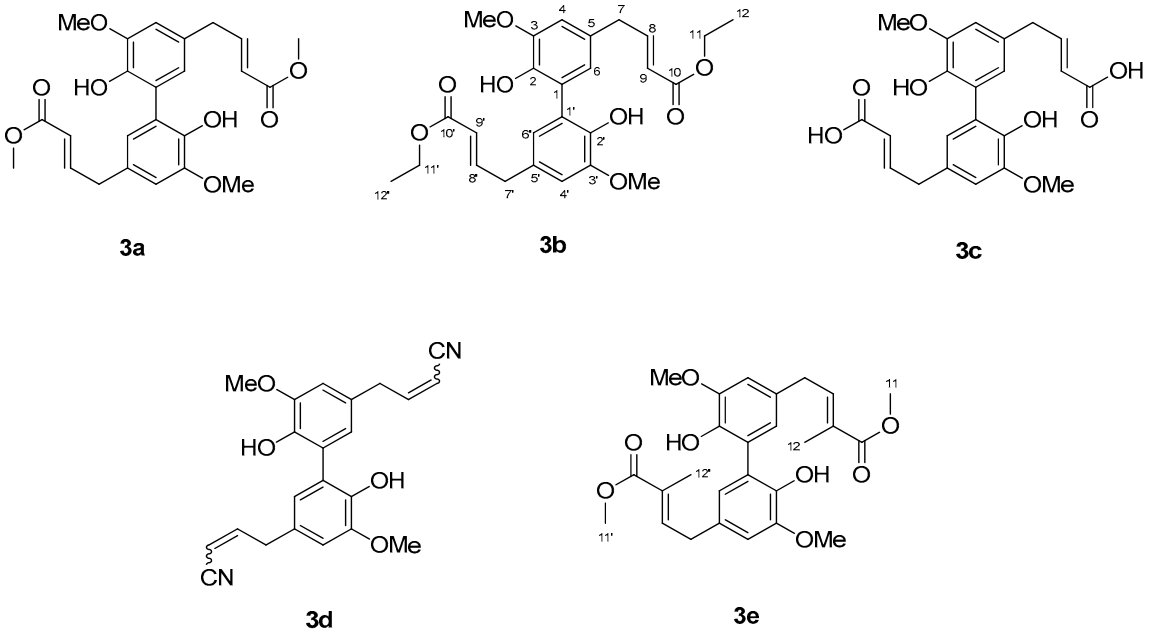

Figure 3. New dehydrodieugenol derivatives **3a**–**3e** resulting from cross metathesis with acrylic olefins and **1**.

To the best of our knowledge, compounds **3a**–**3e** shown in Figure 3 are described herein for the first time. Based on the anti-*Trypanosoma cruzi* effect observed with compound **1**, these new products were tested against trypomastigote and amastigote forms of this parasite. As summarized in Table 3, it was noticed that the modification in the structure of compound **1** via cross metathesis reaction resulted in compounds with no detectable toxicity to the highest tested concentration (CC_{50} values > 200 μM for **3a**–**3e** against a value

of 58.2 μM for compound **1** and with potential against trypomastigote forms of parasite displaying IC_{50} values ranging from 11.6 to 79.5 μM. However, as described by the DNDi (Drugs for Neglected Diseases initiative), activity against intracellular (amastigote) forms of parasite is crucial to the development of new drugs for Chagas disease [55].

Table 3. Anti-*Trypanosoma cruzi* activity and cytotoxicity in mammalian cells of compounds **1** and **3a–3e**.

Compound	IC_{50}/μM		CC_{50}/μM	SI	
	Trypomastigote	Amastigote	NCTC	Trypomastigote	Amastigote
1	11.5 ± 2.5	15.1 ± 3.4	58.2	3.9	3.8
3a	19.9 ± 0.1	NA	>200	>10.0	-
3b	11.9 ± 0.7	17.7 ± 8.0	>200	>16.8	>11.2
3c	79.5 ± 9.3	NA	>200	>2.5	-
3d	23.5 ± 2.0	15.5 ± 1.8	>200	>8.5	>12.9
3e	11.6 ± 2.1	NA	>200	>17.2	-
benznidazole	5.5 ± 0.9	18.7 ± 4.1	>200	>36.4	>10.7

IC_{50}—50% inhibitory concentration; CC_{50}—50% cytotoxic concentration; SI—selectivity index, calculated by the ratio CC_{50} against NCTC cells/IC_{50} against parasites (trypomastigote and amastigote forms); NA: not active.

As also observed in Table 3, among all tested compounds, derivatives **3b** and **3d** exhibited activity against amastigotes with IC_{50} values of 17.7 and 15.5 μM. Considering the reduced toxicity of both compounds, the SI values were determined as >11.2 and >12.9, respectively, similar to the standard drug benznidazole (IC_{50} of 18.7 μM and SI > 10.7). Chemically, these data suggest that the insertion of an ethoxycarbonyl group (**3b**) and a cyanide (**3d**) group in the original structure of starting material **1** plays an important role in reducing toxicity on NCTC cells and maintaining anti-amastigote activity. Interestingly, the presence of methoxycarbonyl group (**3a** and **3e**) or free carboxylic acid (**3c**) afforded inactive compounds. Therefore, compounds **3b** and **3d** can be considered as a promising starting point for the development of new prototypes for future drug discovery studies for Chagas disease [31].

3. Materials and Methods

3.1. General Experimental Procedures

All reactions were conducted under an inert atmosphere of argon using standard Schlenk tube techniques. Solvents were dried by distillation or using a MBraun Solvent purification system prior to use. Dimethyl carbonate and diethyl carbonate were distilled under atmospheric pressure and stored under argon over activated 3 Å molecular sieves. Eugenol (99%) and hydrochloric acid (>37%) were purchased from Sigma-Aldrich, St. Gallen, Switzerland and used as received. Hoveyda Grubbs II catalyst (97%) was supplied by Umicore AG, Germany and used without further purification. Ethyl acrylate (99%), ammonium hydroxide solution (28–30%), acrylic acid (99%), and potassium hexacyanoferrate (III) (99%) were purchased from Alfa-Aesar, Le Mans, France and used without further purification. Methyl acrylate, methyl methacrylate, and anhydrous sodium sulfate were purchased from Acros Organics, Illkirch, France. Methyl acrylate and methyl methacrylate were stored under argon over activated 3 Å molecular sieves prior to use. Acrylonitirile was distilled under atmospheric pressure and stored under argon over activated 3 Å molecular sieves. Acetone, dimethylformamide, and anhydrous potassium carbonate (99%) were purchased from Fischer Chemical, Illkirch-Graffenstaden, France. Silica gel (0.040–0.063 mm) from Macherey-Nagel, Hœrdt, France was used for column chromatography, while silica gel (60 Å) from Merck, Darmstadt, Germany was used for analytical TLC. NMR spectra were recorded on a Bruker model Avance III, Wissemburg, Germany, operating at 400 MHz (^{1}H) and 100 MHz (^{13}C), and on a Varian 500, Palo Alto, CA, USA, operating at 500 MHz (^{1}H) and 125 MHz (^{13}C), while featuring spectrometers using $CDCl_3$ or DMSO-d_6 as solvent. ESI-HRMS spectra were measured on an Agilent 6510 QTOF LC/MS spectrometer, Santa Clara, CA, USA.

3.2. Preparation of Dehydrodieugenol (**1**)

Preparation of dehydrodieugenol **1** was performed based on the methodology previously reported [46]. A saturated aqueous solution of $K_3[Fe(CN)_6]$ (3.29 g in 14.5 mL of H_2O, 10 mmol, 1 equiv.) was slowly transferred into a flask containing a solution of eugenol (1.64 g, 10 mmol, 1 equiv.) in 16 mL of acetone, 8 mL of distillated H_2O and 25 mL of $NH_3{\cdot}H_2O$ (25%). The mixture was kept under magnetic stirring for 5 h at room temperature. Then, $NH_3{\cdot}H_2O$ was neutralized with concentrated HCl (22 mL) until the formation of a precipitate, which was washed three times with distillated H_2O and recrystallized using absolute EtOH.

Dimethoxy-5,5′-diprop-2-enyl [1,1′-biphenyl]-2,2′-diol (biseugenol) **1**

Colorless crystalline plates. ^{1}H NMR Figure S1 (400 MHz, $CDCl_3$, δ ppm) 6.75 (2H, d, *J* = 1.6 Hz, H-6/6′), 6.67 (2H, d, *J* = 1.6 Hz, H-4/4′), 5.99 (2H, s, 2- and 2′-OH), 5.98 (2H, ddt, *J* = 17.0, 10.1 and 6.7 Hz, H-8/H8′), 5.11 (2H, dd, *J* = 17.0 and 1.7 Hz, H-9a/H-9′a), 5.07 (2H, dd, *J* = 10.1 and 1.7 Hz, H-9b/H-9′b), 3.92 (s, 6H, 3- and 3′-OCH_3), 3.36 (4H, d, *J* = 7.6 Hz, 2 × CH_2). ^{13}C NMR (100 MHz, $CDCl_3$, δ ppm) 147.3 (C-2/C-2′), 141.1 (C-3/C-3′), 137.8 (C-8/C-8′), 132.1 (C-5/C-5′), 124.5 (C-1/C-1′), 123.3 (C-6/C-6′), 115.9 (C-9/C-9), 110.8 (C-4/C-4′), 56.2 (C-10/C-10′), 40.1 (C-7/C-7′). ESI-HRMS *m*/*z* 349.1418 $[M + Na]^+$ (calculated for $C_{20}H_{22}O_4Na$, 349.1416). These values are consistent with the data described in the literature [46].

3.3. General Procedure for Cross Metathesis Reactions

In a first study, several olefins were tested as metathesis partners in the modification of compound **1** according to conditions described in Table 1. In general, reactions were conducted in a dry and degassed Schlenk tube loaded under argon with 50 mg of compound **1** (0.15 mmol), 1.9 mg of **Ru1** (3×10^{-3} mmol, 2 mol%), and 1.6 mg of *p*-benzoquinone (1.5×10^{-2} mmol, 10 mol%). A second study was performed using methyl acrylate as olefin metathesis partner and compound **1** as substrate aiming at optimizing the reaction conditions (Table 1). The variation of the *p*-benzoquinone amount (in the absence or in the presence of 1.5×10^{-3} mmol, 10 mol%) was performed in overnight tests. Variation of the amount of **Ru1** catalyst (3–6 × 10^{-3} mmol, 2–4 mol%), solvent (2–10 mL), and methyl acrylate (**2a**, 0.61–1.86 mmol, 4–12 equiv.) was performed in a slow addition of the catalyst (0.25 mL h^{-1}) procedure, as described: a dry and degassed Schlenk tube was loaded under argon with 50 mg of compound **1** (0.15 mmol), *p*-benzoquinone, and methyl acrylate (**2a**), and then closed by a rubber septum. Another dry and degassed Schlenk tube was loaded under argon with Hoveyda-Grubbs II catalyst and 0.5 mL of solvent. This solution was pumped into a 1 mL syringe and then slowly added into the first Schlenk tube through the septum by means of a syringe-pump for 2 h. After addition, the reaction mixture was stirred at 80 °C for an additional 3 h. In both procedures (overnight and slow addiction of catalyst), the solvent evaporation was performed and the products were purified by chromatography column on silica gel using heptane/EtOAc mixtures. After defining the best metathesis conditions for the different olefin partners, compounds **3a**–**3e** were prepared in a dry and degassed Schlenk tube loaded under argon with 50 mg of compound **1**, *p*-benzoquinone (10 mol%), and the selected olefin as follows:

i. methyl acrylate (**2a**, 56 µL) to afford compound **3a**
ii. ethyl acrylate (**2b**, 65 µL) to afford compound **3b**
iii. acrylic acid (**2c**, 42 µL) to afford compound **3c**
iv. acrylonitrile (**2d**, 40 µL) to afford compound **3d**
v. methyl methacrylate (**2e**, 2 mL) to afford compound **3e**

Hoveyda-Grubbs II catalyst (2 mol%) was slowly added during 2 h (0.25 mL/h) under stirring using a syringe-pump and the reaction proceeded for more than three hours. After solvent evaporation, the products were purified by chromatography column over silica gel using a mixture of heptane/EtOAc.

3.3.1. (9. *E*,9′*E*)-dimethyl 7,7′-(2,2′-dihydroxy-3,3′-dimethoxy-[1,1′-biphenyl]-5,5′-diyl)bis(but-9-enoate), **3a**

Yellowish oil (yield 52%). ^{1}H NMR (400 MHz, $CDCl_3$, δ ppm) 7.10 (2H, dt, *J* = 15.6 and 6.8 Hz, H-8/H-8′), 6.72 (2H, d, *J* = 1.8 Hz, H-6/H-6′), 6.68 (2H, d, *J* = 1.8 Hz, H-4/H-4′), 5.98 (2H, s, 2- and 2′-OH), 5.86 (2H, d, *J* = 15.6 Hz, H-9/H-9′), 3.91 (6H, s, 3- and 3′-OCH_3), 3.72 (6H, s, H-11/H-11′), 3.49 (4H, d, *J* = 6.8 Hz, H-7/H-7′). ^{13}C NMR (100 MHz, $CDCl_3$, δ ppm) 167.1 (C-10/C-10′), 147.9 (C-8/C-8′), 147.5 (C-2/C-2′), 141.6 (C-3/C-3′), 129.5 (C-5/C-5′), 124.5 (C-1/C-1′), 123.5 (C-6/C-6′), 121.9 (C-9/C-9′), 110.9 (C-4/C-4′), 56.3 (C-11/C-11′), 51.6 (3- and 3-OCH_3), 38.4 (C-7/C-7′). ESI-HRMS *m*/*z* 465.1520 $[M + Na]^+$ (calculated for $C_{24}H_{26}O_8Na$, 465.1525).

3.3.2. (9. *E*,9′*E*)-diethyl 7,7′-(2,2′-dihydroxy-3,3′-dimethoxy-[1,1′-biphenyl]-5,5′-diyl)bis(but-2-enoate) **3b**

Yellowish oil (yield 25%). ^{1}H NMR (400 MHz, $CDCl_3$, δ ppm) 7.09 (2H, dt, *J* = 15.5 and 6.8 Hz, H-8/H-8′), 6.73 (2H, d, *J* = 1.8 Hz, H-6/H-6′), 6.69 (2H, d, *J* = 1.8 Hz, H-4/H-4′), 6.00 (2H, s, 2- and 2′-OH), 5.85 (2H, d, *J* = 15.5 Hz, H-9/H-9′), 4.18 (4H, q, *J* = 7.1 Hz, H-11/H-11′), 3.92 (6H, s, 3- and 3′-OCH_3), 3.49 (4H, d, *J* = 6.8 Hz, H-7/H-7′), 1.27 (6H, t, *J* = 7.1 Hz, H-12/H-12′). ^{13}C NMR (100 MHz, $CDCl_3$, δ ppm) 166.7 (C-10/C-10′), 147.6 (C-8/C-8′), 147.5 (C-2/C-2′), 141.6 (C-3/C-3′), 129.6 (C-5/C-5′), 124.5 (C-1/C-1′), 123.5 (C-6/C-6′), 122.2 (C-9/C-9′), 111.0 (C-4/C-4′), 60.4 (C-11/C-11′), 56.3 (3- and 3′-OCH_3), 38.4 (C-7/C-7′), 14.4 (C-12/C-12′). ESI-HRMS *m*/*z* 493.1835 $[M + Na]^+$ (calculated for $C_{26}H_{30}O_8Na$, 493.1838).

3.3.3. (9. *E*,9′*E*)-7,7′-(2,2′-dihydroxy-3,3′-dimethoxy-[1,1′-biphenyl]-5,5′-diyl)bis(but-2-enoic acid) **3c**

Brownish amorphous solid (yield 32%). ^{1}H NMR (500 MHz, DMSO-d_6, δ ppm) 8.24 (s, 2H, 2- and 2′-OH), 6.91 (2H, dt, *J* = 15.5 and 7.0 Hz, H-8/H-8′), 6.78 (2H, d, *J* = 1.8 Hz, H-6/H-6′), 6.54 (2H, d, *J* = 1.8 Hz, H-4/H-4′), 5.78 (2H, d, *J* = 15.5 Hz, H-9/H-9′), 3.80 (6H, s, 3- and 3′-OCH_3), 3.43 (4H, d, *J* = 7.0 Hz, H-7/H-7′). ^{13}C NMR (125 MHz, DMSO-d_6, δ ppm) 167.1 (C-10/C-10′), 148.0 (C-8/C-8′), 147.8 (C-2/C-2′), 142.2 (C-3/C-3′), 128.0 (C-5/C-5′), 125.9 (C-1/C-1′), 123.1 (C-6/C-6′), 122.1 (C-9/C-9′), 111.1 (C-4/C-4′), 55.9 (4- and 4′-OCH_3), 37.2 (C-7/C-7′). ESI-HRMS *m*/*z* 437.1209 $[M + Na]^+$ (calculated for $C_{22}H_{22}O_8Na$ 437.1212).

3.3.4. 7,7′-(2,2′-dihydroxy-3,3′-dimethoxy-[1,1′-biphenyl]-5,5′-diyl)bis(but-2-enenitrile) **3d**

Yellowish oil (yield 51%). ^{1}H NMR (400 MHz, $CDCl_3$, δ ppm) (*Z*)-3d: 6.75 (2H, d, *J* = 1.7 Hz, H-6/H-6′), 6.73 (2H, d, *J* = 1.7 Hz, H-4/H-4′), 6.63 (2H, dt, *J* = 10.8 and 7.7 Hz, H-8/H-8′), 5.98 (2H, s, 2- and 2′-OH), 5.39 (2H, d, *J* = 10.8 Hz, H-9/H-9′), 3.93 (6H, s, 3- and 3′-OCH_3), 3.72 (4H, d, *J* = 7.6 Hz, H-7/H-7′). (*E*)-3d: 6.89 (2H, dt, *J* = 16.3 and 6.5 Hz, H-8/H-8′), 6.69 (2H, d, *J* = 1.7 Hz, H-6/H-6′), 6.65 (2H, d, *J* = 1.7 Hz, H-2/H-2′), 5.97 (2H, s, 2- and 2′-OH), 5.33 (2H, dt, *J* = 16.2 and 1.6 Hz, H-9/H-9′), 3.93 (6H, s, 3- and 3′-OCH_3), 3.51 (4H, d, *J* = 6.5 Hz, H-7/H-7′). ^{13}C NMR (100 MHz, $CDCl_3$, δ ppm) (Z)-3d: 153.2 (C-8/C-8′), 147.5 (C-2/C-2′), 141.8 (C-3/C-3′), 128.6 (C-1/C-1′), 124.4 (C-6/C-6′), 123.1 (C-5/C-5′), 116.1 (C-10/C-10′), 110.7 (C-4/C-4′), 99.7 (C-9/C-9′), 56.3 (3- and 3′-OCH_3), 37.8 (C-7/7′). (E)-3d: 154.3 (C-8/C-8′), 147.5 (C-2/C-2′), 141.9 (C-3/C-3′), 127.7 (C-1/C-1′), 124.3 (C-6/C-6′), 123.5 (C-5/C-5′), 117.4 (C-10/C-10′), 110.8 (C-4/C-4′), 100.8 (C-9/C-9′), 56.3 (3- and 3′-OCH_3), 39.1 (C-7/C-7′). ESI-HRMS *m*/*z* 399.1313 $[M + Na]^+$ (calculated for $C_{22}H_{20}N_2O_4Na$, 399.1321).

3.3.5. (9. *E*,9′*E*)-dimethyl 7,7′-(2,2′-dihydroxy-3,3′-dimethoxy-[1,1′-biphenyl]-5,5′-diyl)bis(9-methylbut-9-enoate) **3e**

Yellowish oil (yield 29%). ^{1}H NMR (400 MHz, $CDCl_3$, δ ppm) 6.93 (2H, t, *J* = 7.5 Hz, H-8/H-8′), 6.72 (2H, br s, H-6/H-6′), 6.70 (2H, br s, H-4/H-4′), 5.96 (2H, s, 2- and 2′-OH), 3.92 (6H, s, 3- and 3′-OCH_3), 3.73 (6H, s, H-11/H-11′), 3.49 (4H, d, *J* = 7.5 Hz, H-7/H-7′), 1.95 (6H, s, H-12/H-12′). ^{13}C NMR (100 MHz, $CDCl_3$, δ ppm) 168.7 (C-10/C-10′), 147.5 (C-2/C-2′), 141.4 (C-3/C-3′), 140.8 (C-6/C-6′), 130.9 (C-1/C-1′), 128.1 (C-9/C-9′), 124.5

(C-5/C-5′), 123.1 (C-8/C-8′), 110.7 (C-4/C-4′), 56.3 (3- and 3′-OCH_3), 51.9 (C-11/C-11′), 34.8 (C-7/C-7′), 12.7 (C-12/C-12′). ESI-HRMS m/z 493.1829 $[M + Na]^+$ (calculated for $C_{26}H_{30}O_8Na$, 493.1838).

3.4. Experimental Animals

BALB/c mice were obtained by the animal breeding facility at the Instituto Adolfo Lutz—São Paulo, SP, Brazil. The animals were maintained in sterilized boxes with absorbent material under a controlled environment and received water and food ad libitum. BALB/c mice were used to obtain peritoneal macrophages and for *T. cruzi* maintenance infection. Animal procedures were performed with the approval of the Research Ethics Commission (project CEUA-IAL 05/2018), in agreement with the Guide for the Care and Use of Laboratory Animals from the National Academy of Sciences.

3.5. Parasites and Mammalian Cell Maintenance

Trypanosoma cruzi trypomastigotes (Y strain) were maintained in Rhesus monkey kidney cells (LLC-MK2—ATCC CCL 7), using RPMI-1640 medium supplemented with 2% FBS at 37 °C in a 5% CO_2-humidified incubator. The murine conjunctive cells (NCTC clone 929, ATCC) and LLC-MK2 were maintained in RPMI-1640 supplemented with 10% FBS at 37 °C in a 5% CO_2—humidified incubator. Macrophages were obtained from the peritoneal cavity of BALB/c mice by washing them with RPMI—1640 medium supplemented with 10% FBS and were maintained at 37 °C in a 5% CO_2-humidified incubator.

3.6. Determination of Anti-Trypomastigote and Anti-Amastigote Activity

The 50% inhibitory concentration (IC_{50}) of tested compounds **3a**–**3e** against *T. cruzi* was determined in trypomastigotes and amastigotes forms. Trypomastigotes were obtained from LLC-MK2 cultures previously infected. The parasites were counted in a Neubauer hemocytometer, seeded at 1×10^6 cells/well (96-well plates), and incubated with serial dilutions of the tested compounds **3a**–**3e** (1.71–150 μM) for 24 h at 37 °C in a 5% CO_2-humidified incubator, with benznidazole as the standard drug. The trypomastigote viability was evaluated by the resazurin (Sigma) assay [56]. To determine the activity against intracellular amastigotes, peritoneal macrophages from BALB/c mice were infected with trypomastigotes forms of *T. cruzi.* The macrophages obtained from the peritoneal cavity of BALB/c mice were plated on a 16-well chamber slide (NUNC plate, Thermo; 1×10^5/well) and incubated for 24 h at 37 °C in a 5% CO_2-humidified incubator. Trypomastigotes obtained as described above were washed in RPMI-1640 medium, and then counted and used to infect the macrophages (parasite to macrophage ratio = 10:1). After an incubation for 2 h at 37 °C in a 5% CO_2-humidified incubator, residual free parasites were removed by washing with medium. Next, tested compounds were incubated with infected macrophages (48 h at 37 °C, 5% CO_2) at different concentrations using benznidazole as the standard drug. At the end of the assay, slides were fixed with MeOH and stained with Giemsa prior to counting under a light microscope. The IC_{50} values were calculated as previously described [56].

3.7. Determination of Cytotoxicity against Mammalian Cells

Cytotoxicity was performed in mice fibroblasts NCTC cells-clone L929. The cells (6×10^4 cells/well) were seeded and individually incubated with tested compounds **3a**–**3e** (1.56–200 μM) for 48 h at 37 °C in a 5% CO_2 incubator. The 50% cytotoxic concentration (CC_{50}) was determined by MTT assay [57]. The optical density was determined in FilterMax F5 (Molecular Devices) at 570 nm. The selectivity index (SI) values were calculated for both forms of the parasite (trypomastigotes and amastigotes) using the equation: CC_{50} against NCTC cells/IC_{50} against parasites.

3.8. Statistical Analysis

All data were expressed as mean ± SEM. Comparisons between groups were made using ANOVA followed by Newman-Keuls correction factor as a post-test. The GraphPad Prism program, version 6.0, was used to perform statistical analysis and graph construction. For p values < 0.05, the differences between means were considered significant.

4. Conclusions

Five new compounds have been synthesized by cross metathesis of biseugenol (**1**) with electron deficient olefins. The products resulting from the reactions with acrylates and acrylic acid present almost perfect (*E*)-configuration, whereas a mixture of (*Z*) and (*E*)-isomers with the (*Z*)-isomer as the major product was obtained from acrylonitrile. These compounds were characterized by NMR and HRMS techniques and their biological activity was evaluated against *Trypanosoma cruzi*. Among all the synthesized compounds, higher potency against *T. cruzi* was obtained for compounds **3b** and **3d** with IC_{50} values of 17.7 and 15.5 μM, respectively, to amastigote forms of the parasite. Contrasting to the starting material **1**, these compounds exhibited no mammalian toxicity (CC_{50} > 200 μM) with elevated SI values. Based on these results, compounds **3b** and **3d** can be considered promising materials for future studies of Chagas disease.

Supplementary Materials: The following supporting information can be downloaded at: https://www.mdpi.com/article/10.3390/catal13071097/s1, Figure S1. ^{1}H NMR (δ, $CDCl_3$, 400 MHz) of **1**; Figure S2. ^{13}C NMR (δ, $CDCl_3$, 100 MHz) of **1**; Figure S3. ESI-HRMS (positive mode) of **1**; Figure S4. ^{1}H NMR (δ, $CDCl_3$, 400 MHz) of **3a**; Figure S5. ^{13}C NMR (δ, $CDCl_3$, 100 MHz) of **3a**; Figure S6. ESI-HRMS (positive mode) of **3a**; Figure S7. ^{1}H NMR (δ, $CDCl_3$, 400 MHz) of **3b**; Figure S8. ^{13}C NMR (δ, $CDCl_3$, 100 MHz) of **3b**; Figure S9. ESI-HRMS (positive mode) of **3b**; Figure S10. ^{1}H NMR (δ, $CDCl_3$, 500 MHz) of **3c**; Figure S11. ^{13}C NMR (δ, $CDCl_3$, 125 MHz) of **3c**; Figure S12. ESI-HRMS (positive mode) of **3c**; Figure S13. ^{1}H NMR (δ, $CDCl_3$, 400 MHz) of **3d**; Figure S14. ^{13}C NMR (δ, $CDCl_3$, 100 MHz) of **3d**; Figure S15. ESI-HRMS (positive mode) of **3d**; Figure S16. ^{1}H NMR (δ, $CDCl_3$, 400 MHz) of **3e.** Figure S17. ^{13}C NMR (δ, $CDCl_3$, 100 MHz) of **3e**; Figure S18. ESI-HRMS (positive mode) of **3e**; Figure S19. ^{1}H NMR (δ, $CDCl_3$, 400 MHz) of **4e** - mono cross metathesis of **1** with methyl methacrylate (**2e**).

Author Contributions: Conceptualization, W.A.C., J.H.G.L., D.M., C.F. and C.B.; methodology, T.S.G., M.M.G., A.K.U., W.A.C., T.A.C.-S., M.B.A., A.G.T., J.H.G.L., D.M., C.F. and C.B.; formal analysis, T.S.G., M.M.G., A.K.U., W.A.C., T.A.C.-S., M.B.A., A.G.T., J.H.G.L., D.M., C.F. and C.B.; investigation, T.S.G., M.M.G., A.K.U., T.A.C.-S. and M.B.A.; resources, W.A.C., A.G.T., J.H.G.L., D.M., C.F. and C.B.; writing—original draft preparation, T.S.G., A.G.T., J.H.G.L., D.M., C.F. and C.B.; writing—review and editing, J.H.G.L., D.M., C.F. and C.B.; supervision, J.H.G.L., D.M., C.F. and C.B.; project administration, J.H.G.L., D.M., C.F. and C.B.; funding acquisition, J.H.G.L., D.M., C.F. and C.B. All authors have read and agreed to the published version of the manuscript.

Funding: The authors thank CAPES−COFECUB (project PHC 884-17-France; 883/2017-Brazil) for financial support and a post-doctoral fellowship to TSG (process 88887.198050/2018-00). They are also grateful to Umicore AG for the supply of Hoveyda catalyst M72. Authors are also thankful for the financial support and fellowships provided by Coordenação de Aperfeiçoamento de Pessoal de Nível Superior—Brasil (CAPES, Finance Code 001), Conselho Nacional de Desenvolvimento Científico e Tecnológico (CNPq, for grants to OS, AGT and JHGL) and to Fundação de Amparo à Pesquisa do Estado de São Paulo (FAPESP 2021/02789-7, 2021/04464-8, 2018/07885-1, 2017/50333-7 and 2018/10279-6). D.M. and W.A.C thank projects CNPq (312288/2019-0, 422290/2016-5, and 404843/2018-2), FAPESP (2018/01258-5 and 2021/12342-0) and the Sustainable Technologies Unit of UFABC (NuTS).

Data Availability Statement: Data is contained within the article or supplementary material.

Acknowledgments: We are thankful for the technical support of the Federal University of ABC, Instituto Adolfo Lutz, and Université de Rennes.

Conflicts of Interest: We wish to confirm that there are no known conflict of interest associated with this publication and that there has been no significant financial support for this work that could have influenced its outcome.

References

1. Crane, E.A.; Gademann, K. Capturing biological activity in natural product fragments by chemical synthesis. *Angew. Chem. Int. Ed.* **2016**, *55*, 3882–3902. [CrossRef]
2. Szychowski, J.; Truchon, J.-F.; Bennani, Y.L. Natural Products in Medicine: Transformational Outcome of Synthetic Chemistry. *J. Med. Chem.* **2014**, *57*, 9292–9308. [CrossRef]
3. Newman, D.J.; Cragg, G.M. Natural Products as Sources of New Drugs over the 30 Years from 1981 to 2010. *J. Nat. Prod.* **2012**, *75*, 311–335. [CrossRef]
4. Wenqiang, G.; Shufen, L.; Ruixiang, Y.; Shaokun, T.; Can, Q. Comparison of essential oils of clove buds extracted with supercritical carbon dioxide and other three traditional extraction methods. *Food Chem.* **2007**, *101*, 1558–1564.
5. Juhász, L.; Kürti, L.; Antus, S. Simple Synthesis of Benzofuranoid Neolignans from *Myristica fragrans*. *J. Nat. Prod.* **2000**, *63*, 866–870. [CrossRef] [PubMed]
6. Delogu, G.; Fabbri, D.; Dettori, M.A.; Forni, A.; Casalone, G. Enantiopure 2,2′-dihydroxy-3,3′-dimethoxy-5,5′-diallyl-6,6′-dibromo-1,1′-biphenyl: A conformationally stable C2-dimer of a eugenol derivative. *Tetrahedron Asymmetry* **2004**, *15*, 275–282. [CrossRef]
7. Fujisawa, S.; Kashiwagi, Y.; Atsumi, T.; Iwakura, I.; Ueha, T.; Hibino, Y.; Yokoe, I. Application of bis-eugenol to a zinc oxide eugenol cement. *J. Dent.* **1999**, *27*, 291–295. [CrossRef] [PubMed]
8. Barratt, M.D.; Basketter, D.A. Possible origin of the skin sensitization potential of isoeugenol and related compounds. *Contact Dermat.* **1992**, *27*, 98–104. [CrossRef] [PubMed]
9. Takeyoshi, M.; Noda, S.; Yamazaki, S.; Kakishima, H.; Yamasaki, K.; Kimber, I. Assessment of the skin sensitization potency of eugenol and its dimers using a non-radioisotopic modification of the local lymph node assay. *J. Appl. Toxicol.* **2004**, *24*, 77–81. [CrossRef]
10. Gerosa, R.; Borin, M.; Menegazzi, G.; Puttini, M.; Cavalleri, G. In vitro evaluation of the cytotoxicity of pure eugenol. *J. Endod.* **1996**, *22*, 532–534. [CrossRef]
11. De Diaz, A.M.; Gottlieb, H.E.; Gottlieb, O.R. Dehydrodieugenols from Ocotea cymbarum. *Phytochemistry* **1980**, *19*, 681–682. [CrossRef]
12. Ogata, M.; Hoshi, M.; Urano, S.; Endo, T. Antioxidant Activity of Eugenol and Related Monomeric and Dimeric Compounds. *Chem. Pharm. Bull.* **2000**, *48*, 1467–1469. [CrossRef]
13. Bortolomeazzi, R.; Verardo, G.; Liessi, A.; Callea, A. Formation of dehydrodiisoeugenol and dehydrodieugenol from the reaction of isoeugenol and eugenol with DPPH radical and their role in the radical scavenging activity. *Food Chem.* **2010**, *118*, 256–265. [CrossRef]
14. Murakami, Y.; Shoji, M.; Hanazawa, S.; Tanaka, S.; Fujisawa, S. Preventive effect of bis-eugenol, a eugenol ortho dimer, on lipopolysaccharide-stimulated nuclear factor kappa B activation and inflammatory cytokine expression in macrophages. *Biochem. Pharmacol.* **2003**, *66*, 1061–1066. [CrossRef] [PubMed]
15. Murakami, Y.; Shoji, M.; Hirata, A.; Tanaka, S.; Yokoe, I.; Fujisawa, S. Dehydrodiisoeugenol, an isoeugenol dimer, inhibits lipopolysaccharide-stimulated nuclear factor kappa B activation and cyclooxygenase-2 expression in macrophages. *Arch. Biochem. Biophys.* **2005**, *434*, 326–332. [CrossRef]
16. Fujisawa, S.; Ishihara, M.; Yokoe, I. Computer-Aided Synthesis of Dimerized Eugenol. *Int. Elec. J. Mol. Des.* **2004**, *3*, 241–246.
17. Shen, J.-L.; Man, K.-M.; Huang, P.-H.; Chen, W.-C.; Chen, D.-C.; Cheng, Y.-W.; Liu, P.-L.; Chou, M.-C.; Chen, Y.-H. Honokiol and Magnolol as Multifunctional Antioxidative Molecules for Dermatologic Disorders. *Molecules* **2010**, *15*, 6452–6465. [CrossRef]
18. Mascia, M.P.; Fabbri, D.; Dettori, M.A.; Ledda, G.; Delogu, G.; Biggio, G. Hydroxylated biphenyl derivatives are positive modulators of human GABAA receptors. *Eur. J. Pharmacol.* **2012**, *693*, 45–50. [CrossRef]
19. Wu, L.; Zou, H.; Xia, W.; Wang, L. Role of magnolol in the proliferation of vascular smooth muscle cells. *Herz* **2015**, *40*, 542–548. [CrossRef]
20. Kleiner, H.E.; Vulimiri, S.V.; Miller, L.; Johnson, W.H., Jr.; Whitman, C.P.; DiGiovanni, J. Oral administration of naturally occurring coumarins leads to altered phase I and II enzyme activities and reduced DNA adduct formation by polycyclic aromatic hydrocarbons in various tissues of SENCAR mice. *Carcinogenesis* **2001**, *22*, 73–82. [CrossRef] [PubMed]
21. Ho, K.-Y.; Tsai, C.-C.; Chen, C.-P.; Huang, J.-S.; Lin, C.-C. Antimicrobial activity of honokiol and magnolol isolated from Magnolia officinalis. *Phytother. Res.* **2001**, *15*, 139–141. [CrossRef] [PubMed]
22. Wang, X.; Wang, Y.; Geng, Y.; Li, F.; Zheng, C. Isolation and purification of honokiol and magnolol from cortex Magnoliae officinalis by high-speed counter-current chromatography. *J. Chromatogr. A* **2004**, *1036*, 171–175. [CrossRef] [PubMed]
23. Lin, Y.-R.; Chen, H.-H.; Ko, C.-H.; Chan, M.-H. Effects of honokiol and magnolol on acute and inflammatory pain models in mice. *Life Sci.* **2007**, *81*, 1071–1078. [CrossRef]
24. Wang, J.-H.; Shih, K.-S.; Liou, J.-P.; Wu, Y.-W.; Chang, A.S.-Y.; Wang, K.-L.; Tsai, C.-L.; Yang, C.-R. Anti-Arthritic Effects of Magnolol in Human Interleukin 1β-Stimulated Fibroblast-Like Synoviocytes and in a Rat Arthritis Model. *PLoS ONE* **2012**, *7*, e31368. [CrossRef] [PubMed]

25. Jada, S.; Doma, M.R.; Singh, P.P.; Kumar, S.; Malik, F.; Sharma, A.; Khan, I.A.; Qazi, G.N.; Kumar, H.M.S. Design and synthesis of novel magnolol derivatives as potential antimicrobial and antiproliferative compounds. *Eur. J. Med. Chem.* **2012**, *51*, 35–41. [CrossRef]
26. Ikeda, K.; Nagase, H. Magnolol Has the Ability to Induce Apoptosis in Tumor Cells. *Biol. Pharm. Bull.* **2002**, *25*, 1546–1549. [CrossRef]
27. Xu, H.; Tang, W.; Du, G.; Kokudo, N. Targeting apoptosis pathways in cancer with magnolol and honokiol, bioactive constituents of the bark of Magnolia officinalis. *Drug Discov. Ther.* **2011**, *5*, 202–210. [CrossRef]
28. Miyazawa, M.; Hisama, M. Antimutagenic Activity of Phenylpropanoids from Clove (*Syzygium aromaticum*). *J. Agric. Food Chem.* **2003**, *51*, 6413–6422. [CrossRef]
29. Okada, N.; Hirata, A.; Murakami, Y.; Shoji, M.; Sakagami, H.; Fujisawa, S. Induction of cytotoxicity and apoptosis and inhibition of cyclooxygenase-2 gene expression by eugenol-related compounds. *Anticancer Res.* **2005**, *25*, 3263–3269.
30. Cho, W.C.-S. Nasopharyngeal carcinoma: Molecular biomarker discovery and progress. *Mol. Cancer* **2007**, *6*, 1. [CrossRef]
31. Grecco, S.S.; Costa-Silva, T.A.; Jerz, G.; de Sousa, F.S.; Conserva, G.A.A.; Mesquita, J.T.; Galuppo, M.K.; Tempone, A.G.; Neves, B.J.; Andrade, C.H.; et al. Antitrypanosomal activity and evaluation of the mechanism of action of dehydrodieugenol isolated from *Nectandra leucantha* (Lauraceae) and its methylated derivative against *Trypanosoma cruzi*. *Phytomedicine* **2017**, *24*, 62–67. [CrossRef]
32. Higman, C.S.; Lummiss, J.A.M.; Fogg, D.E. Olefin metathesis at the dawn of implementation in pharmaceutical and specialty-chemicals manufacturing. *Angew. Chem. Int. Ed.* **2016**, *55*, 3552–3565. [CrossRef]
33. Van Lierop, B.J.; Lummiss, J.A.M.; Fogg, D.E. *Olefin Metathesis, Theory and Practice*; Grela, K., Ed.; Wiley: Hoboken, NJ, USA, 2014; pp. 85–152.
34. Cossy, J. Applications of olefin metathesis reactions: Applications in the synthesis of natural products and biologically active molecules. In *Olefin Metathesis, Theory and Practice*; Grela, K., Ed.; Wiley & Sons Inc.: Hoboken, NJ, USA, 2014; pp. 287–309.
35. Cossy, J.; Willis, C.; Bellosta, V. Enantioselective allyltitanation and cross metathesis. synthesis of (−)-prosophylline. *Synlett* **2001**, *10*, 1578–1580. [CrossRef]
36. Van Zijl, A.W.; Szymanski, W.; López, F.; Minnaard, A.J.; Feringa, B.L. Catalytic Enantioselective Synthesis of Vicinal Dialkyl Arrays. *J. Org. Chem.* **2008**, *73*, 6994–7002. [CrossRef] [PubMed]
37. Bressin, R.K.; Osman, S.; Pohorilets, I.; Basu, U.; Koide, K. Total Synthesis of Meayamycin B. *J. Org. Chem.* **2020**, *85*, 4637–4647. [CrossRef]
38. Li, J.; Ahmed, T.S.; Xu, C.; Stoltz, B.M.; Grubbs, R.H. Concise Syntheses of Δ^{12}-Prostaglandin J Natural Products via Stereoretentive Metathesis. *J. Am. Chem. Soc.* **2019**, *141*, 154–158. [CrossRef]
39. Brummer, O.; Ruckert, A.; Blechert, S. Olefin cross metathesis with monosubstituted olefins. *Chem. Eur. J.* **1997**, *3*, 441–446. [CrossRef]
40. Bilel, H.; Hamdi, N.; Fischmeister, C.; Bruneau, C. Transformations of bio-sourced 4-hydroxyphenylpropanoids based on olefin metathesis. *ChemCatChem* **2020**, *12*, 5000–5021. [CrossRef]
41. Zaja, M.; Blechert, S. Concise enantioselective synthesis of (−)-lasubine II. *Tetrahedron* **2004**, *60*, 9629–9634. [CrossRef]
42. Bilel, H.; Hamdi, N.; Zagrouba, F.; Fischmeister, C.; Bruneau, C. Eugenol as a renewable feedstock for the production of polyfunctional alkenes via olefin cross metathesis. *RSC Adv.* **2012**, *2*, 9584–9589. [CrossRef]
43. Vieira, G.M.; Granato, A.V.; Gusevskaya, E.V.; dos Santos, E.N.; Dixneuf, P.H.; Fischmeister, C.; Bruneau, C. Tandem hydroformylation/isomerization/hydrogenation of bio-derived 1-arylbutadienes for the regioselective synthesis of branched aldehydes. *Appl. Catal. A Gen.* **2020**, *598*, 117583. [CrossRef]
44. Dixneuf, P.H.; Bruneau, C.; Fischmeister, C. Alkene Metathesis Catalysis: A Key for Transformations of Unsaturated Plant Oils and Renewable Derivatives. *Oil Gas Sci. Technol.* **2016**, *71*, 19. [CrossRef]
45. Galhardo, T.S.; Ueno, A.K.; Costa-Silva, T.A.; Tempone, A.G.; Carvalho, W.A.; Fischmeister, C.; Bruneau, C.; Mandelli, D.; Lago, J.H.G. New derivatives from dehydrodieugenol B and its methyl ether displayed high anti-*Trypanosoma cruzi* activity and cause depolarization of the plasma membrane and collapse the mitochondrial membrane potential. *Chem. Biol. Interact.* **2022**, *366*, 110129. [CrossRef]
46. Rodrigues, L.C.; Barbosa-Filho, J.M.; de Oliveira, M.R.; Néris, P.L.N.; Borges, F.V.P.; Mioso, R. Synthesis and Antileishmanial Activity of Natural Dehydrodieugenol and Its Mono- and Dimethyl Ethers. *Chem. Biodivers.* **2016**, *13*, 870–874. [CrossRef]
47. Garber, S.B.; Kingsbury, J.S.; Gray, B.L.; Hoveyda, A.H. Efficient and recyclable monomeric and dendritic Ru-based metathesis catalysts. *J. Am. Chem. Soc.* **2000**, *122*, 8168–8179. [CrossRef]
48. Hassam, M.; Taher, A.; Arnott, G.E.; Green, I.R.; van Otterlo, W.A.L. Isomerization of allylbenzenes. *Chem. Rev.* **2015**, *115*, 5462–5569. [CrossRef] [PubMed]
49. Miao, X.; Fischmeister, C.; Bruneau, C.; Dixneuf, P.H. Dimethyl Carbonate: An Eco-Friendly Solvent in Ruthenium-Catalyzed Olefin Metathesis Transformations. *Chemsuschem* **2008**, *1*, 813–816. [CrossRef] [PubMed]
50. Miao, X.; Dixneuf, P.H.; Fischmeister, C.; Bruneau, C. A green route to nitrogen-containing groups: The acrylonitrile cross metathesis and applications to plant oil derivatives. *Green Chem.* **2011**, *13*, 2258–2271. [CrossRef]
51. Miao, X.; Malacea, R.; Fischmeister, C.; Bruneau, C.; Dixneuf, P.H. Ruthenium–alkylidene catalysed cross metathesis of fatty acid derivatives with acrylonitrile and methyl acrylate: A key step toward long-chain bifunctional and amino acid compounds. *Green Chem.* **2011**, *13*, 2911–2919. [CrossRef]

52. Bidange, J.; Fischmeister, C.; Bruneau, C.; Dubois, J.-L.; Couturier, J.-L. Cross metathesis of bio-sourced fatty nitriles with acrylonitrile. *Monatsh. Chem.* **2015**, *146*, 1107–1113. [CrossRef]
53. Bruneau, C.; Fischmeister, C.; Miao, X.; Malacea, R.; Dixneuf, P.H. Cross metathesis with acrylonitrile and applications to fatty acid derivatives. *Eur. J. Lipid Sci. Technol.* **2010**, *112*, 3–9. [CrossRef]
54. Torker, S.; Koh, M.J.; Khan, R.K.M.; Hoveyda, A.H. Regarding a persisting puzzle in olefin metathesis with ru complexes: Why are transformations of alkenes with a small substituent Z-selective? *Organometallics* **2016**, *35*, 543–562. [CrossRef]
55. Don, R.; Ioset, J.-R. Screening strategies to identify new chemical diversity for drug development to treat kinetoplastid infections. *Parasitology* **2014**, *141*, 140–146. [CrossRef]
56. Rea, A.; Tempone, A.G.; Pinto, E.G.; Mesquita, J.T.; Rodrigues, E.; Silva, L.G.M.; Sartorelli, P.; Lago, J.H.G. Soulamarin Isolated from *Calophyllum brasiliense* (Clusiaceae) Induces Plasma Membrane Permeabilization of *Trypanosoma cruzi* and Mytochondrial Dysfunction. *PLoS Neglected Trop. Dis.* **2013**, *7*, e2556. [CrossRef] [PubMed]
57. Tada, H.; Shiho, O.; Kuroshima, K.; Koyama, M.; Tsukamoto, K. An improved colorimetric assay for interleukin 2. *J. Immunol. Methods* **1986**, *93*, 157–165. [CrossRef]